Synthesis and Characterization of A New Conjugated Aromatic Poly(azomethine) Derivative Based on the 3′,4′-Dibutyl-α-Terthiophene Building Block

Chenggang Wang, Seaver Shieh, Eugene LeGoff, and Mercouri G. Kanatzidis*,†

Department of Chemistry and the Center for Fundamental Materials Research, Michigan State University, East Lansing, Michigan 48824

Received September 19, 1995; Revised Manuscript Received January 25, 1996⊗

ABSTRACT: A new conjugated aromatic poly(azomethine) derivative, poly(3′,4′-dibutyl-α-terthiophene−azomethine-1,4-phenylene−azomethine) (PBTPI), has been prepared by polycondensation of 2,5″-diformyl-3′,4′-dibutyl-2,2′:5′,2″-terthiophene with 1,4-phenylenediamine under the ethanothermal conditions. The red polycrystalline PBTPI was characterized by X-ray diffraction, NMR, FTIR, UV−visible−near-IR, photoluminescence, and ESR spectroscopies. PBTPI is partially soluble in tetrahydrofuran, giving an orange solution with an absorption maximum (λ_{max}) of 457 nm. In the solid state, PBTPI has an optical band gap of 2.06 eV, which is one of the lowest among poly(azomethines), and is highly sensitive to a strong acid environment. Protonation yields a blue polymer with an optical band gap of 1.61 eV. The polymer is completely soluble in concentrated sulfuric acid and nitromethane containing Lewis acids (e.g., $AlCl_3$), giving blue solutions with λ_{max} of 656 and 638 nm, respectively. Iodine-doped PBTPI shows low electrical conductivity at the order of 10^{-7}−10^{-8} S/cm. The properties of PBTPI are compared to other, previously characterized, related polymers.

Introduction

Conjugated polymers have gained widespread interest during the last two decades, because of their useful electronic, optoelectronic, electrochemical, and nonlinear optical properties.[1,2] Among conjugated polymers, those with extended π systems involving alternating C=C and C−C bonds are predominant. This is the case for many prototypical conjugated polymers, such as polyacetylene,[3] poly(*p*-phenylene),[4] and poly(*p*-phenylene−vinylene).[5] Because the CH=N group is isoelectronic with the CH=CH group, the incorporation of nitrogen atoms into the conjugated system is another approach to form classes of materials with equally interesting electronic and optical properties. Polyaniline is a well-known example, which is constructed by the alternating *p*-phenylene rings and nitrogen atoms in the polymer backbone.[6] Polyaniline shows unique features such as nonoxidizing doping by protonation[7] and the dependence of the degree of oxidation and properties on the fraction of two types nitrogen atoms, i.e., imine (=N, sp^2) and amine (>N, sp^3). Polyazines, $[-N=C(R)C(R)=N-]_x$ (R = H, alkyl), have also received attention recently.[8−10] The polyazine, $[-N=CHCH=N-]_x$, is formally isoelectronic with polyacetylene, $[-CH=CHCH=CH-]_x$, but unlike polyacetylene, it is very stable in air.[8] Polyazines are synthesized via acid-catalyzed condensation reactions between an α,β-dihydrazone and an α,β-dicarbonyl. They can be doped with iodine to give air-stable, electrically conducting, materials with room temperature conductivity as high as 1.3 S/cm.[8]

Conjugated poly(azomethines), polyimines, or poly(Schiff bases) are another interesting class of conjugated polymers containing nitrogen atoms in a polymer backbone. The first poly(azomethines) were prepared by Adams and co-workers from terephthalaldehyde and benzidine and dianisidine in 1923.[11] The basic aromatic conjugated poly(azomethine) is poly(1,4-phenylenemethylidynenitrilo-1,4-phenylenenitrilomethylidyne)[12] (PPI), which is isoelectronic with poly(*p*-phenylene−vinylene) (PPV). Unlike PPV, the imine nitrogen of the PPI backbone introduces additional useful features and chemical flexibility,[12−19] including high solubility in concentrated sulfuric acid and the complexation with Lewis acids.

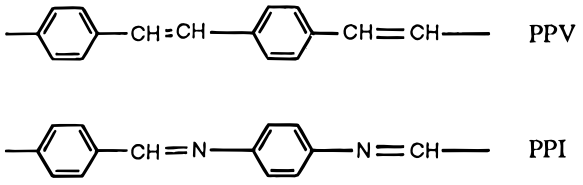

A major obstacle to characterizing and developing most conjugated aromatic poly(azomethines) has been their intractability and insolubility in common organic solvents. Several methods have been reported to improve the processability of conjugated poly(azomethines) by modification and selection of polymer structure, for example, unsymmetrical[17] or symmetrical[18] substitutions in the main-chain aromatic benzene rings with flexible alkyl or alkoxy side chains. A recent approach based on the reversible Lewis acid−base complexation has also been successfully applied to the processing of nonsubstituted and substituted poly(azomethines).[19] Poly(azomethines) possess optical band gaps in the range 2.03−2.83 eV.

Recently, we reported the synthesis and characterization of a new soluble and dopable conjugated copolymer consisting of 3′,4′-dibutyl-2,2′:5′,2″-terthiophene and phenylene vinylene units,[20a] i.e., poly(3′,4′-dibutyl-2,2′:5′,2″-terthiophene-1,2-ethenylene-1,4-phenylene-1,2-ethenylene) (PBTPV). Exploiting the Wittig reac-

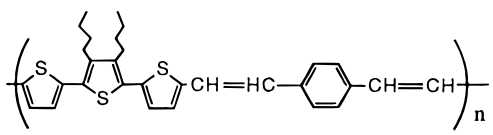

PBTPV

† Camille and Henry Dreyfus Teacher Scholar.
⊗ Abstract published in *Advance ACS Abstracts,* March 15, 1996.

0024-9297/96/2229-3147$12.00/0

tions of 2,5″-diformyl-3′,4′-dibutyl-2,2′:5′,2″-terthiophene (DFDBT) with various appropriate bis(ylides) gives several other interesting new copolymers.[20b] These materials show "tunable" physicochemical properties while maintaining the enhanced solubility imparted by the 3′,4′-dibutyl-2,2′:5′,2″-terthiophene (DBTT) building block. As a natural extension of this research, we have synthesized a new conjugated aromatic poly(azomethine), i.e. poly(3′,4′-dibutyl-α-terthiophene−azomethine−1,4-phenylene−azomethine) (PBTPI), by using the poly-

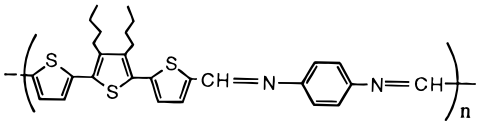

PBTPI

condensation reaction between the dialdehyde derivative of the terthiophene (DFDBT) and 1,4-phenylenediamine under ethanothermal condition.[21] PBTPI is formally isoelectronic with the PBTPV. To our knowledge, this is the first alkyl-substituted oligothiophene-linked conjugated poly(azomethine).[22] It is notable that the replacement of a phenylene linkage by a thiophene linkage in the polyquinolines or polyanthrazoline backbone shows a significant reduction of solid-state band gap by 0.3−0.5 eV.[23] Substitution of the benzene ring with a 3′,4′-dibutyl-2,2′:5′,2″-terthiophene building block in conjugated poly(azomethine) systems should not only improve the solubility but also further reduce the band gap of the resulting polymer. The preparation and physicochemical characterization including XRD, FTIR, UV−visible−near-IR, and NMR of this new conjugated poly(azomethine) are described herein. The properties of the new poly(azomethines) are compared with other known related polymers.

Experimental Section

Materials. 1,4-Phenylenediamine (97% purity) was used as received from Aldrich Chemical Co., Inc. Ethanol was distilled from CaH_2 and stored over 4-Å Linde molecular sieves before use. Acetone was used as received from commercial sources. Tetrahydrofuran (THF; HPLC grade) and 1-methyl-2-pyrrolidinone (NMP; HPLC grade) were used as received from Aldrich Chemical Co., Inc. without further purification. Protic acids such as HCl, HNO_3, and H_2SO_4 were purchased from commercial sources and used as received. Deuterated nitromethane (CD_3NO_2-d_3, 99%) was used as received from Cambridge Isotope Laboratories. Anhydrous aluminum trichloride was purchased from EM Science, (Gibbstown, NJ) used and stored under dry glovebox filled with nitrogen.

Synthesis of 2,5″-Diformyl-3′,4′-dibutyl-2,2′:5′,2″-terthiophene (DFDBT). BuLi (2.8 mL of 1.6 M in hexane solution, 2.2 equiv) was added to a cooled (−50 °C) mixture of 3′,4′-dibutyl-2,2′,5′,2″-terthiophene[24] (720 mg, 2.0 mmol), tetramethylethenediamine (TMEDA, 400 mg), and 40 mL of hexane by a syringe under N_2. The reaction mixture was then stirred at −50 °C for 30 min and then again at room temperature for another 30 min. This was followed by cooling to −78 °C and the slow addition of 2.2 equiv of DMF in 5 mL of ether with a syringe. The reaction mixture was slowly warmed to room temperature, stirred for 1 h and then poured into 200 mL of 2% ice cold aqueous HCl solution with vigorous stirring. The mixture was extracted with CH_2Cl_2 (4 × 30 mL), and the combined organic layers were washed with water, saturated sodium bicarbonate, and brine and then dried with $MgSO_4$. Removal of the solvent, with a rotary evaporator, gave a dark-colored residue as the crude product. Chromatographic column purification over silica gel with hexane−ether−CH_2Cl_2 (65/20/15) as the eluent gave the expected DFDBT, as orange needles. Yield: 0.674 g (81%). Mp = 92−93 °C (uncorrected). ^{1}H NMR ($CDCl_3$): ppm 9.91 (s, 2H), 7.73 (d, J = 4.5 Hz, 2H), 7.27 (d, J = 4.5 Hz, 2H), 2.78 (t, J = 8.9 Hz, 4H), 1.54 (m, 4H), 1.48 (m, 4H), 0.97 (t, J = 7.9 Hz, 6H). ^{13}C NMR($CDCl_3$): ppm 13.8, 22.9, 28.0, 32.5, 126.7, 130.5, 136.7, 142.8, 142.9, 145.6, 182.6. EI-MS (e/z, relative intensity): 418 ($M^+ + 2$), 16.4, 417 ($M^+ + 1$, 25.2), 416 (M^+, base), 345 (23.9), 331 (7.3), 303 (42.0), 288 (6.1), 275 (5.6), 270 (5.5), 240 (6.6), 227 (5.6), 127 (6.6), 41 (7.1). UV−visible ($CDCl_3$): maximum absorption (λ_{max}) 404 nm.

Synthesis of Poly(3′,4′-dibutyl-α-terthiophene−azomethine−*p*-phenylene−azomethine) (PBTPI). In a heavy-wall (4-mm thickness) Pyrex tube (∼3 mL) were loaded 0.052 g (0.125 mmol) of the dialdehyde DFDBT, 0.017 g (0.150 mmol) of 1,4-phenylenediamine, and ∼0.5 mL of anhydrous ethanol. The loaded tube was frozen in liquid nitrogen and flame-sealed under a vacuum of $\sim 1.0 \times 10^{-3}$ Torr. The sealed tube was heated in an oven at 125 °C for 24 h. The red solid formed was isolated and washed exhaustively with acetone to remove residual starting materials and oligomers and then dried in vacuo at 50 °C for 24 h. Yield: 0.060 g, 98%. Anal. Calcd (%) for $C_{28}H_{28}N_2S_3$ (repeat unit): C, 68.81; H, 5.78; N, 5.73. Found: C, 66.87; H, 5.96; N, 5.92. ^{1}H NMR of PBTPI (in CD_3NO_2-d_3 containing 2 wt % $AlCl_3$): δ (ppm) 11.23, 9.39, 8.53, 7.93, 3.09, 1.66, 1.05. ^{13}C NMR of PBTPI (in CD_3NO_2-d_3 containing 2 wt % $AlCl_3$): δ (ppm) 157.96, 155.72, 149.55, 138.61, 134.83, 132.11, 131.55, 127.15, 123.63, 32.93, 29.66, 24.04, 14.23. The density of PBTPI is ∼1.26 g/cm^3, as determined by flotation density measurements using a mixed-solvent system of CCl_4 (d = 1.583 g/cm^3) and cyclohexane (d = 0.774 g/cm^3). We note, however, that this value most likely represents a lower bound since the polymer particles contain pores which may not be filled completely by solvent during the flotation experiment.

Synthesis of Protonated PBTPI. (a) Reaction with HCl Vapor. The red PBTPI (0.020 g) on a glass substrate was exposed to the HCl fume from a concentrated HCl solution (12 N) by bubbling nitrogen for 20 min. The red solid became dark blue instantly. The yield was quantitative.

(b) Reaction with Concentrated HCl Solution. The red PBTPI (0.020 g) was stirred with 20 mL of concentrated HCl solution (12 N) for 4 h. The red solid turned to dark blue instantly. It was collected by suction filtration and air-dried at room temperature. The yield was quantitative.

Synthesis of Iodine-Doped PBTPI. (a) Doping with Iodine Vapor. A solution (THF) cast film of the PBTPI on a quartz slide was put into a closed chamber filled with iodine crystals and stored for 4 h. The original orange film turned to dark brown.

(b) Doping with Iodine in Acetonitrile. To a stirred 25-mL 0.1 M iodine acetonitrile solution, 0.012 g of red solid of the PBTPI was added. The red powder turned black immediately. After stirring for 10 h, the black solid was collected, washed several times with acetonitrile, and vacuum-dried at room temperature overnight. The yield was quantitative. The sample was pressed into pellets for electrical conductivity measurements.

Physicochemical Methods. Carbon, hydrogen, and nitrogen elemental analyses were performed by Oneida Research Services Inc. (Whitesboro, NY). Elemental analyses (semi-quantitative) for sulfur and iodine were performed on a JEOL JSM-6400V scanning electron microscope (SEM) equipped with a Tracor Northern energy dispersive spectroscopy (EDS) detector. The molecular weight of the polymer was estimated by the gel permeation chromatography method (relative to polystyrene standards, M_w in the range of 1320−500800) with Shimadzu LC-10AS liquid chromatography equipped with a PL-GEL 5μ MIXC column of length 300 mm, using THF as an eluent at room temperature. We note that the use of polystyrene standards to evaluate the M_w of rodlike polymers is tenuous and should be used with caution and for comparison purposes only. Infrared spectra were obtained in the transmission mode with a Nicolet IR-44 FT-IR spectrometer, in the form of pressed KBr pellets. UV−visible−near-IR absorption

spectra (either in absorption or diffuse reflectance mode) were obtained from a Shimadzu UV-3101PC double-beam, double-monochromator spectrophotometer. Nuclear magnetic resonance spectra (^{1}H and ^{13}C) were obtained at room temperature using a computer-controlled Varian Gemini-NMR (300 MHz) spectrometer. The chemical shifts are reported in parts per million (δ, ppm) using the residual solvent resonance peak as reference (CD_3NO_2, δ 4.33 ppm for ^{1}H and 62.8 ppm for ^{13}C). Solution photoluminescence spectra were measured in dilute THF solution on a Hitachi F-4500 fluorescence spectrophotometer at room temperature. Solid-state photoluminescence spectra were obtained on a SPEX fluorolog-2 (Model F111A1) spectrofluorometer at both 298 (23 °C) and 77 K (-196 °C, liquid nitrogen). Powdered samples were loaded in 3-mm quartz tubing and sealed under vacuum ($\sim 1.0 \times 10^{-4}$ Torr). X-ray powder diffraction patterns were collected at room temperature on a Rigaku powder diffractometer, Rigaku-Denki/RW400F2 (Rotaflex), using Cu(Kα) radiation generated by a rotating anode operating at 45 kV and 100 mA. The data were collected at a scan rate of 0.5 deg/min. The observed *d* spacings were corrected according to an internal standard (Si metal). Thermogravimetric analysis (TGA) and differential scanning calorimetry were performed on Shimadzu TGA-50 and DSC-50 under nitrogen or oxygen at 5 °C/min heating and cooling rate. Electron spin resonance (ESR) spectra were recorded with a Varian EPR-E4 spectrometer with diphenylpicrylhydrazyl radical as *g* marker ($g = 2.0037$). Cylindrical quartz tubes were employed for powders. The conductivity data were measured by the standard four-probe method on pressed pellets at room temperature. Electrochemistry and cyclic voltammetry were performed with a PAR 273 potentiostat−galvanostat equipped with a PAR RE0091 $X-Y$ recorder as reported earlier.[24b]

Results and Discussion

Polymer Synthesis and Characterization. Polycondensation of the dialdehyde (DFDBT) with 1,4-phenylenediamine was first carried in anhydrous ethanol or dimethyl sulfoxide at room or elevated temperature (e.g., ∼120 °C). However, the resulting materials had low molecular weight, were obtained in low yield, and were accompanied by a lot of unreacted starting materials. To achieve high-quality polymer and higher yield, we adopted the solvothermal method,[21] to carry out the polycondensation reaction. Recently, hydrothermal or solvothermal methods have been extensively and successfully used in the synthesis of unusual, high-crystalline, and high-yield new inorganic materials.[25] Similarly, the polycondensation of the dialdehyde (DFDBT) with 1,4-phenylenediamine can be carried out rapidly without any catalyst in a sealed tube under ethanothermal conditions to give nearly quantitative yield, according to eq 1.

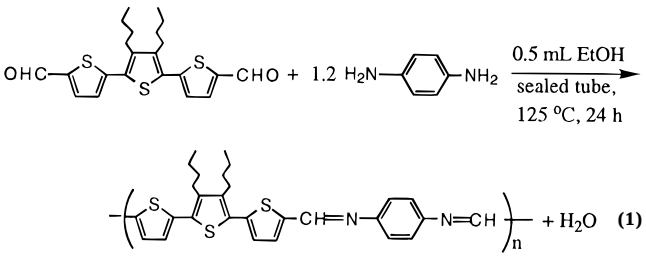

(1)

The resulting conjugated poly(azomethine) PBTPI is a red powder, stable in air and water. The elemental analysis data of the polymer are in good agreement with its expected structure (repeating unit). PBTPI is polycrystalline as determined by the X-ray powder diffraction pattern (see Figure 1). Table 1 lists the observed *d* spacings and relative intensities

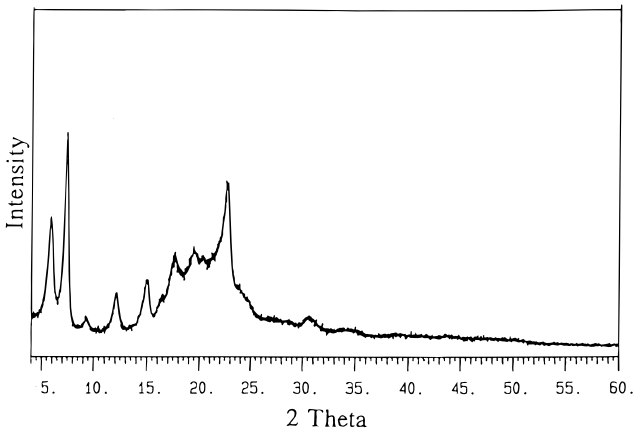

Figure 1. X-ray powder diffraction profile of pristine PBTPI.

Table 1. X-ray Diffraction Data for PBTPI at 23 °C

hkl	d_{obsd} (Å)	d_{calcd} (Å)	intensity$_{obsd}$ (%)
	Orthorhombic Unit Cell[a]		
001	14.82	14.81	62.3
101	11.84	11.83	100.0
111	9.36	9.36	17.7
120	7.24	7.24	28.6
310	5.86	5.86	34.4
022	5.381	5.382	28.0
130	5.034	5.035	46.6
410	4.528	4.532	49.0
303	3.889	3.889	77.7
510	3.682	3.682	30.0

[a] $a = 18.93$ Å, $b = 15.67$ Å, $c = 14.81$ Å, $\beta = 90.0°$, $V = 4393.14$ Å^3, $Z = 8$, $d_{calcd} = 1.48$ g/cm^3.

of the reflection peaks of PBTPI at 23 °C. Although the lattice constants cannot be unambiguously determined with these few reflections, we have attempted to index the peaks to a reasonable unit cell for PBTPI. The observed *d* spacings were corrected using an internal standard of Si powder. Indexing of the reflections was carried out using the TREOR90 and PIRUM programs included in the Cerius^2 molecular simulation software package.[26]

The best solution derived from the indexed reflections is an orthorhombic unit cell with $a = 18.93$ Å, $b = 15.67$ Å, $c = 14.81$ Å, $V = 4393.14$ Å^3. The calculated and observed *d* spacings and the corresponding indices are given in Table 1. The *a* axis of 18.93 Å is close to the length of the repeat unit, ∼18.6 Å, which is calculated from its energy-minimized structure. The polymer chains could lie in parallel to the *a* axis. With the above lattice parameters, the calculated density is ∼1.48 g/cm^3, assuming eight chains per unit cell. It has been reported that the calculated density is 1.33 g/cm^3 for 3′,4′-dibutyl-pentathiophene and 1.26 g/cm^3 for 3′,3‴″,4′,4‴″-tetrabutylhexathiophene.[27] We expect PBTPI to have a slightly higher density than these related oligothiophenes due to its polymeric condensed nature. Furthermore, the PBTPI is expected to possess a lower density than that of polythiophene itself ($d_{calcd} = 1.55$ g/cm^3)[28] because of the presence of *n*-butyl groups on the PBTPI backbone. The experimentally measured density of PBTPI is ∼1.26 g/cm^3, which is a low limit given the porosity of the powder sample and the presence of a certain fraction of amorphous material. Therefore, this density is in good agreement with the calculated one. All other possible unit cells gave unreasonable calculated densities for the material.

Interestingly, neutral PBTPI is highly sensitive to a strong acid environment. Upon exposure to either acid

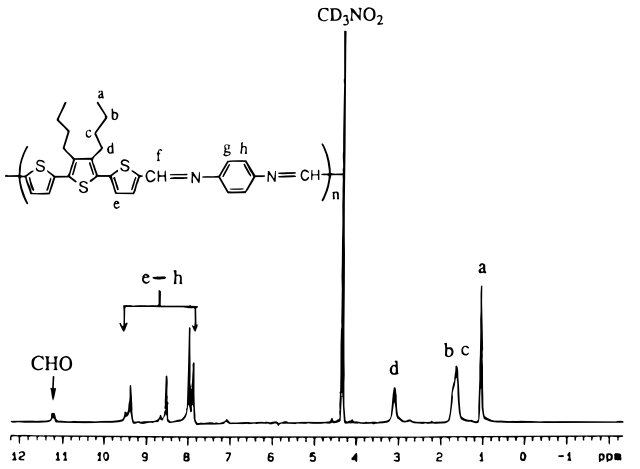

Figure 2. ^{1}H NMR spectrum of PBTPI in CD_3NO_2−$AlCl_3$ and its assignment. Peaks a−d are due to the *n*-butyl groups on the terthiophene block.

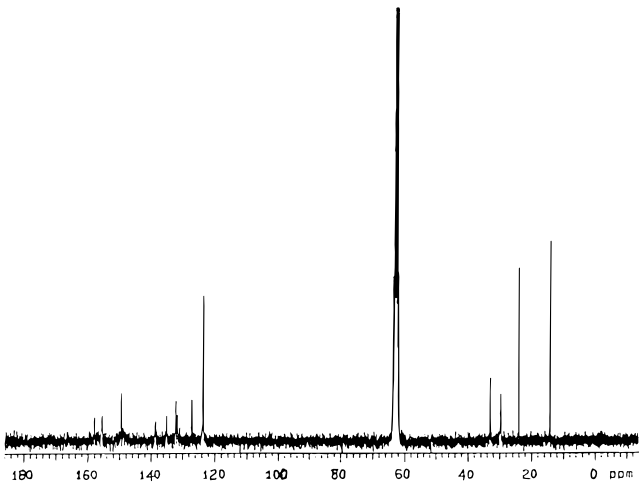

Figure 3. ^{13}C NMR spectrum of PBTPI in CD_3NO_2−$AlCl_3$.

fumes (HCl, HNO_3) or strong acid solution, the red PBTPI (neutral from) undergoes a rapid spectacular change to dark blue (referred as the "protonated form"). The XRD powder patterns of the dark blue materials are very similar to that of pristine PBTPI. The dramatic change of color is accompanied by significant spectroscopic changes, as will be discussed later.

In contrast to PPI, pristine PBTPI is partly soluble in THF, chloroform, and NMP to give orange solutions and a red solid residue. The molecular weight of the soluble fraction can be estimated by GPC using polystyrene standards and THF as an eluent. The weight-average molecular weight ($\bar{M}_w$) is $\sim 3.86 \times 10^3$ and number-average molecular weight ($\bar{M}_n$) is $\sim 2.93 \times 10^3$, giving a polydispersity index of 1.32. The M_n corresponds to an average of six repeat units (24 rings per chain). Because the molecular weights of most poly(azomethines) are reported in their intrinsic viscosities in concentrated H_2SO_4,[19] a direct comparison of the molecular weight of the new polymer with others cannot be made. However, we notice that the soluble fraction has an intermediate molecular weight, while the red insoluble residue is expected to have a much higher average molecular weight.

Similar to PPI and other poly(azomethines),[19] PBTPI is completely soluble in concentrated sulfuric acid and nitromethane containing ~2 wt % aluminum trichloride. The resulting blue solution appears indefinitely stable in air. The enhanced solubility of poly(azomethines) is based on the Lewis acid−base complexation, which has been extensively investigated.[28] The imine nitrogen on the backbone of poly(azomethines) provides a Lewis base site for effecting reversible complexation and solubilization in organic solvents.

NMR Spectroscopy. The ^{1}H NMR and ^{13}C NMR spectra of PBTPI were obtained in deuterated nitromethane containing aluminum trichloride. Figure 2 shows the ^{1}H NMR spectra of PBTPI and its assignment. The number of protons corresponding to each resonance based on integration of the resonances of the NMR spectrum are in good agreement with the proposed structure. The resonance peak at 11.22 ppm is tentatively attributed to the terminal aldehyde, to small amount of residual dialdehyde monomer, or both. This is consistent with the presence of a small peak due to aldehyde groups in the Fourier transform infrared (FTIR) spectrum of the neutral polymer (see below).

The ^{13}C NMR spectrum of PBTPI is shown in Figure 3. It shows four resonance lines in the aliphatic region

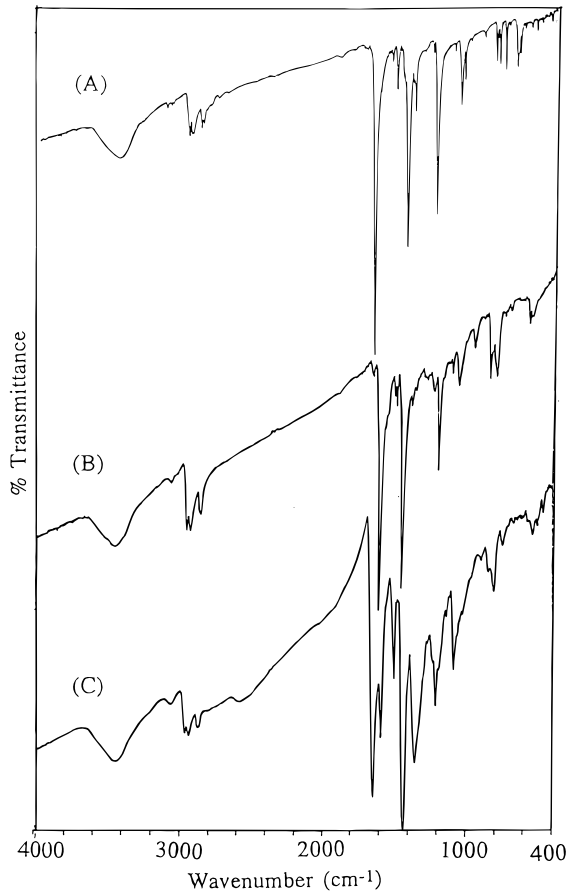

Figure 4. FTIR transmission spectra (KBr pellets) of (A) dialdehyde DFDBT, (B) pristine PBTPI, and (C) protonated (with HCl) PBTPI.

at 32.9, 29.6, 24.0, and 14.2 ppm assigned to the four different carbons of the butyl group. There are nine lines in the aromatic region as would be expected, which correspond to the aromatic carbons on the polymer backbone. The number of resonance peaks in the ^{13}C NMR spectrum in conjunction with the ^{1}H NMR spectrum clearly confirm the proposed structure of the conjugated aromatic PBTPI.

Infrared Spectroscopy. Figure 4 shows the FTIR spectra of the dialdehyde DFDBT, the neutral polymer, and the protonated polymer as KBr pellets (spectra A−C, respectively). The principal FTIR absorption bands observed in the monomer and polymers, their assignments, and data from other known related poly-

Table 2. Comparison of Infrared Band Positions (cm^{-1}) and Their Assignments for PBTPI and Related Polymers

polymer	C=N str	arom $C_{\beta-H}$ str	aliph C−H stretch	ring stretch	methyl def	arom C−H out-of-plane
DFDBT[a]		3063	2955 2934 2853	1539 1508 1431	1381	795
PBTPI-N[b]	1597	3067	2953 2926 2851	1505 1469 1441	1385	798
PBTPI-P[b]	1638	3063	2951 2926 2863	1491 1426		802
PPI[c]	1610					850
PMOPI[c]	1605					840
PHOPI[c]	1600					840−870
PBTPV[d]		3063	2953 2926 2851	1459 1513 1441	1378	804
PDBTT[e]		3062	2951 2925 2856	1492 1456	1377	788

[a] DFDBT, 2,5″-diformyl-3′,4′-dibutyl-2,2′:5′,2″-terthiophene. [b] PBTPI, poly(3′,4′-dibutyl-α-terthiophene−azomethine−1,4-phenylene−azomethine); N, neutral polymer; P, protonated polymer. [c] See ref 19. PPI, poly(1,4-phenylenemethylidynenitrilo−1,4-phenylenenitrilomethylidyne); PMOPI, poly(1,4-phenylenemethylidynenitrilo-2,5-dimethoxy-1,4-phenylene−nitrilomethylidyne); PHOPI, poly(1,4-phenylenemethylidynenitrilo-2,5-dihydroxy-1,4-phenylene−nitrilomethylidyne). [d] See ref 20. PBTPV, poly(3′,4′-dibutyl-2,2′:5′,2″-terthiophene−1,2-ethenylene−1,4-phenylene−1,2-ethenylene). [e] See ref 30. PDBTT, poly(3,4-dibutyl-α-terthiophene).

mers are listed in Table 2. In spectrum A, an absorption band at 1653 cm^{-1} clearly indicates the existence of the aldehyde group in the DFDBT monomer, while in spectrum B, its intensity is drastically decreased. At the same time a new strong absorption band at 1597 cm^{-1} appears which is consistent with the formation of imines (C=N stretching). The strong, sharp absorption band at 1597 cm^{-1} is characteristic of extended conjugated polyazomethines.[19] The new bands at 1194 and 955 cm^{-1} (in spectrum B) are due to the aromatic C−H in-plane deformation vibrations, while the band at 843 cm^{-1} (aromatic C−H out-of-plane deformation) is characteristic of 1,4-disubstituted (para) benzene.[30] The band at 799 cm^{-1} (aromatic C−H out-of-plane deformation) is characteristic of 2,5-coupled thiophene rings as has been observed in PDBTT[24] and other alkyl-substituted polythiophenes.[31] Upon exposure to hydrochloride acid (either vapor or solution), the red polymer turns blue immediately, and this is associated with a profound change in the IR spectrum, as shown in spectrum C. The presence of a broad absorption of medium intensity at 2573 ($N-H^+$ stretching) and 1638 cm^{-1} ($C=NH^+$ stretching) suggests the formation of imine hydrochloride $C=NH^+$[30,32] and, thus, is consistent with protonation by HCl (see Scheme 1). The shift of the C=N stretching band of azomethine or poly(azomethine) toward higher energy, upon protonation or complexation with Lewis acids, has been reported previously in the literature.[19,32] The protonation or complexation with Lewis acids causes a significant change in electronic structure, by means of coordination of a strong electron-withdrawing group to the imine nitrogen (C=N), inducing a redistribution of electron density throughout the material.

The neutral polymer could be regenerated from the protonated form by heating in a vacuum at 100 °C for 24 h or by treating with a base solution. The IR spectrum of the regenerated polymer (red color) is identical to that of the pristine neutral polymer. The protonation and deprotonation processes are completely reversible and can be repeated many times without significant degradation. Estimated from the results of the TGA studies and EDS/SEM microprobe analysis (see below), the level of protonation of the polymer is 1.5 protons per repeating unit (each repeat unit has two possible protonation sites). Additional experimental evidence of this reversible facile protonation and deprotonation includes the dramatic changes in the electronic spectra which will be discussed below.

Electronic Absorption Spectra of the Neutral PBTPI and Complexes. The neutral PBTPI is partly soluble in THF, $CHCl_3$, and NMP, giving orange solutions. The electronic absorption spectra of the soluble

Scheme 1. Proposed Structures of PBTPI: (A) Protonated with HCl and (B) Complexed with $AlCl_3$

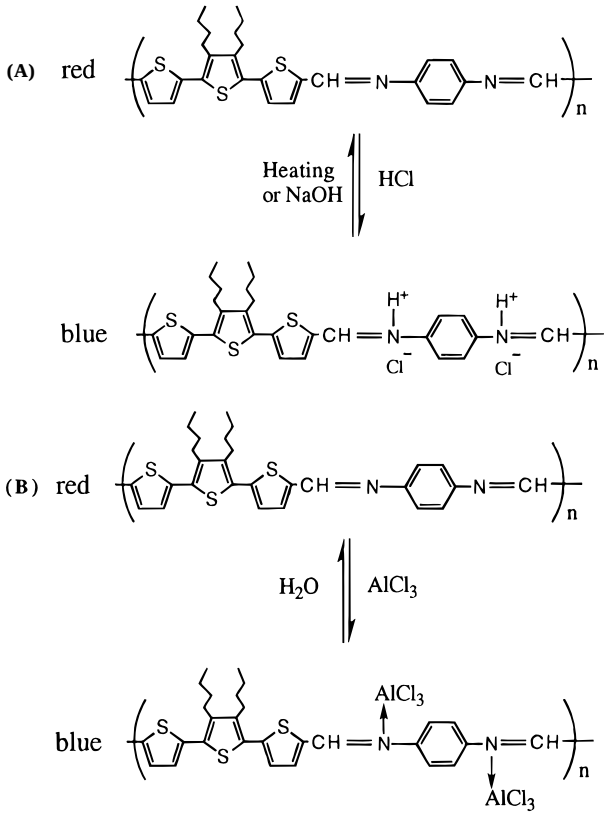

fraction of the polymer in THF or NMP are shown in Figure 5. The absorption maximum (λ_{max}) of the $\pi-\pi^*$ transition in the THF and NMP solution is 457 and 464 nm, respectively. Figure 6 shows the electronic spectra of PBTPI in sulfuric acid and $AlCl_3-CH_3NO_2$. The solution absorption spectra of PBTPI in sulfuric acid and $AlCl_3-CH_3NO_2$ show the λ_{max} of the lowest energy $\pi-\pi^*$ transition at 656 (with an onset of the absorption edge at 1.66 eV) and 638 nm (with an onset of the absorption edge at 1.72 eV), respectively. Those absorption maxima occur at the longest wavelengths among the known conjugated poly(azomethines).[19] For example, the solution electronic spectra of PPI, PMPI, PPI/PMPI, PMOPI, and PHOPI in sulfuric acid show the λ_{max} of the lowest energy $\pi-\pi^*$ transition is in the range of 438−565 nm.[19] Thus, our polymer contains the longest conjugation length in concentrated sulfuric acid.

One notable aspect of the electronic spectra of the PBTPI in sulfuric acid or $AlCl_3-CH_3NO_2$ is their significant red shift compared to the solution spectra of neutral polymers in THF or NMP, which indicates a

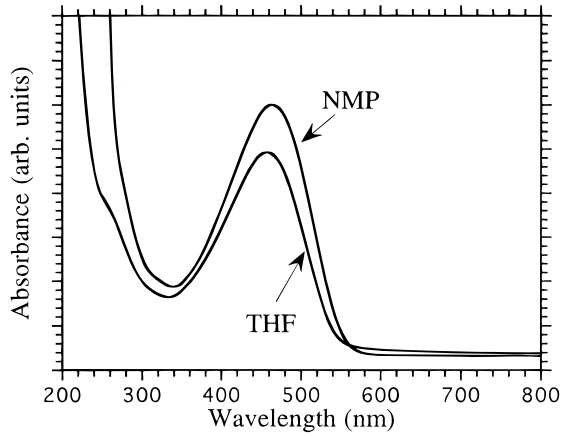

Figure 5. Solution UV−visible absorption spectra of PBTPI in THF (λ_{max} = 457 nm) and NMP (λ_{max} = 464 nm).

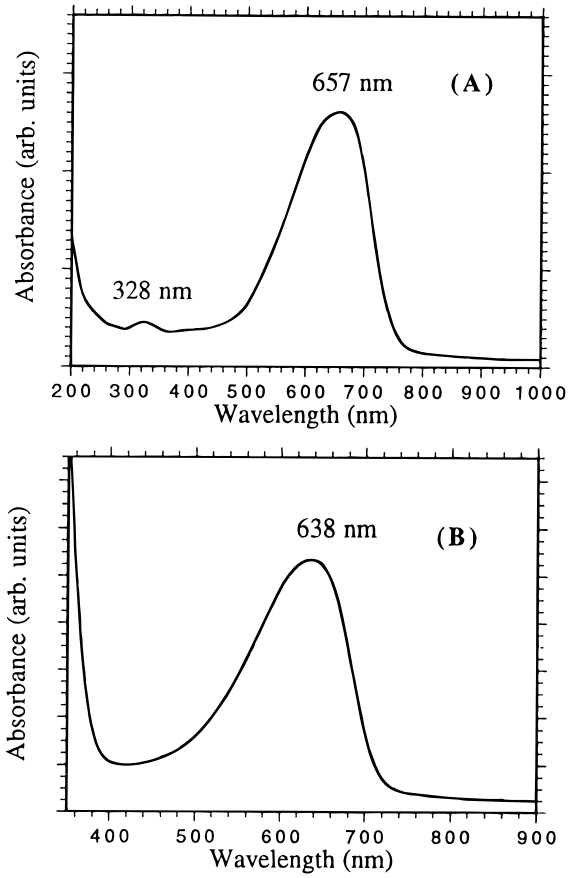

Figure 6. Solution UV−visible absorption spectra of PBTPI in (A) H_2SO_4 and (B) CH_3NO_2 containing ~2 wt % $AlCl_3$.

dramatic change of the polymer electronic structure upon complexation. It is notable that a similar red shift of electronic spectra of some known poly(azomethines) upon complexation has been previously attributed to complexation-induced change in polymer conformation.[19a] We believe conformational changes are not as likely to cause such dramatic shifts in the electronic spectra. These optical changes are likely due to excited-state perturbations by the resonance effect of a strong electron-withdrawing group (e.g., $AlCl_3$), as has been reported in the protonation of Schiff bases.[32] Theoretical calculations show that protonation lowers the energy of π^* orbitals localized on the C=N groups of the Schiff bases but leaves the π orbitals essentially unaltered and, as a result, decreases the HOMO−LUMO gap.[32]

Figure 7 shows the electronic absorption spectra of

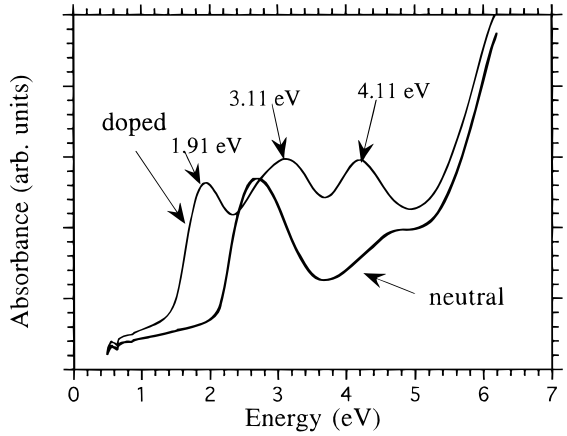

Figure 7. UV−visible−near-IR absorption spectra of the THF solution-cast thin films of PBTPI in (A) neutral form and (B) iodine-doped form.

Table 3. Electronic Absorption Maxima, Absorption Edge (onset), and Solid-State Band Gap of Conjugated Poly(azomethines)

polymer	$\lambda_{max,\ nm}$	absorption edge, (onset) (nm)	E_g (eV)
PBTPI	461	590	2.10[a]
PPI[b]	405	496	2.50
PMPI[b]	406	497	2.49
PMOPI[b]	447	529	2.34
PHOPI[b]	494	600	2.07
PBPI[c]		490	2.53
PSPI[c]		520	2.38
1,5-PNI[c]		495	2.51
PPV[d]	405	512	2.43
PBTPV[e]	450	605	2.05

[a] Value from the THF solution-cast film. Bulk PBTPI has a smaller E_g, ~2.06 eV. [b] Values from ref19a. [c] Values from ref 19b. [d] Values from ref 35. [e] Values from ref 20.

thin films cast from a THF solution of PBTPI. The lowest energy absorption maxima (λ_{max}), the onsets of optical absorption edges, and the corresponding band gaps of the PBTPI (in the solid state) and other related conjugated polymers are summarized in Table 3. The band gap of PBTPI is 2.10 eV with the λ_{max} of 475 nm, as compared to the 2.50-eV (λ_{max} = 405 nm) band gap of the PPI.[19] Recently, it was reported that the replacement of a phenylene linkage by a thiophene linkage in the polyquinoline or polyanthrazoline backbone produced a significant red shift of λ_{max} by 64−106 nm and a reduction of band gap by 0.3−0.5 eV.[23] This effect was attributed to the reduction of steric hindrance and the greater delocalized π-electron density in the thiophene-linked conjugated polymer, which may involve the possible delocalization of the lone pair electrons of the sulfur atom in a thiophene ring. It was known from our previous studies that the dibutyl-substituted terthiophene building block is highly conjugated and less sterically hindered.[24] Thus, the incorporation of the terthiophene units in the conjugated poly(azomethine) backbone could dramatically enhance the coplanarity of the flexible terthiophene rings with the rigid phenylene azomethine ($CH{=}NC_6H_4$) units and improve the π-electron delocalization along the polymer backbone. It has been suggested from theoretical calculations on periodic conjugated block copolymers that the band gap and electronic states of such copolymers are controlled primarily by the contributions of those moieties which give the lower band gap homopolymers.[33] Since the band gap of PBTPI is close to that of the homopolymer PDBTT (e.g., ~2.0 eV), our experimental results seem to support such a theoretical argument.

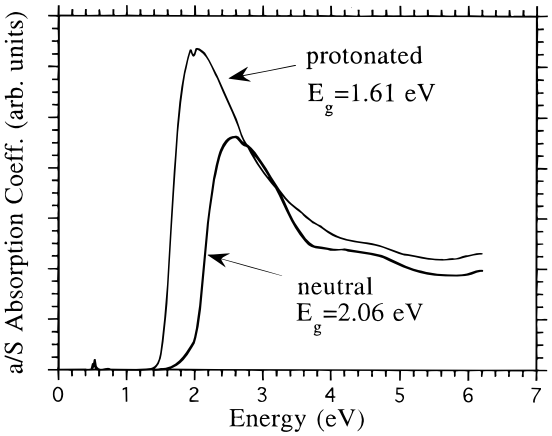

Figure 8. Optical absorption spectra of pristine and protonated (with HCl) bulk PBTPI.

Upon doping with iodine, the solution-cast films turn dark brown. The UV−visible−near-IR absorption spectra of films at the neutral and doped state are compared in Figure 7. The $\pi-\pi^*$ absorption band at 2.69 eV disappears upon oxidation and two new absorption bands appear at higher energy (3.11 and 4.22 eV), and one new low-energy absorption appears at 1.94 eV. These results are different from those of PBTPV and PDBTT, which forms two new subgap absorption bands (formation of bipolaron transitions) upon oxidation by iodine.[20,24]

The optical properties of the bulk polymer (in neutral or protonated form) were also assessed by studying the UV−visible−near-IR diffuse reflectance spectra in the solid state. Absorption data were calculated from the reflectance data using the Kubelka−Munk function.[34] The spectra of the neutral (red) and protonated (blue) forms of bulk PBTPI are shown in Figure 8. From the characteristically steep absorption edges, the band gaps (E_g) of the neutral and protonated PBTPI are estimated at 2.06 and 1.61 eV, respectively. That the polymer has a similar electronic structure in solution as well as solid state is supported by the fact that the band gap of the neutral bulk polymer is only slightly smaller than that of the soluble fraction of the same polymer. The quick reversible response of this material to acid suggests its potential application as a solid-state pH indicator. To test the sensitivity of the polymer to acid, we prepared a thin film (THF solution-cast) of the polymer on a quartz slide and then dipped it into aqueous hydrochloride solutions of various pH values from 7 to 0, for the same amount of time (4 h). Figure 9 shows the change of optical absorbance (monitored at 1.8 eV) as a function of pH. It appears that the polymer only responds to highly acidic media (pH ≥2), which is consistent with the low basicity of the azomethine nitrogen atom.

Photoluminescence Spectroscopy. Figure 10 shows the emission spectrum of the PBTPI in THF solution at 23 °C when excited at 400 nm. Photoexcitation of the polymer in THF solution results in broadband luminescence (half-width ~0.22 eV) with a peak maximum at 2.26 eV (548 nm). In the solid state, the bulk polymer emits orange light at 608 nm when excited at 400 nm at 23 °C (see Figure 11A). The broad tail toward longer wavelength suggests the presence of longer polymer chains. The excitation spectrum shows a peak at 576 nm when emission wavelength is monitored at 655 nm. At 77 K the emission spectrum shows two peaks at 605 and 647 nm, while the excitation

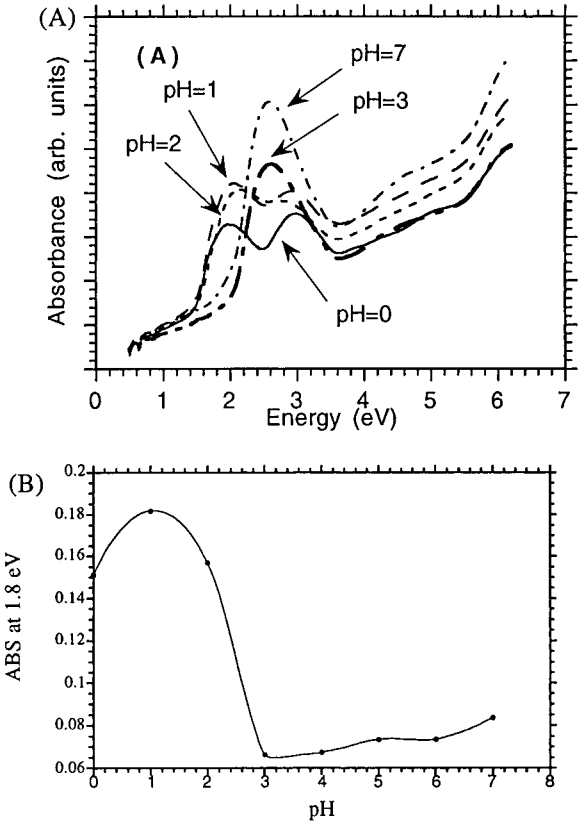

Figure 9. (A) UV−visible−near-IR absorption spectra of THF solution-cast thin films of PBTPI treated with HCl solution at various pH values. (B) A plot of absorbance at 1.8 eV vs pH.

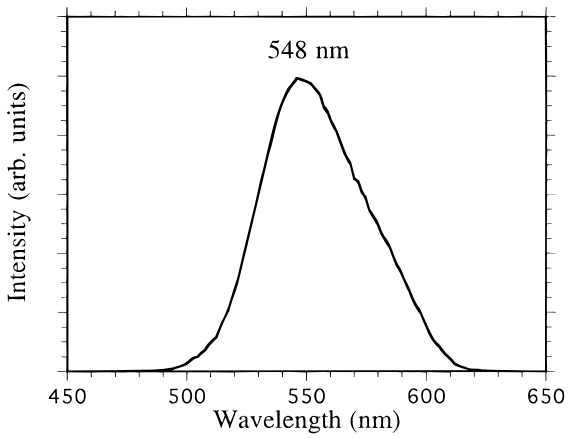

Figure 10. Photoluminescence spectrum of PBTPI in THF solution at room temperature.

spectrum shows a peak at 582 nm, when monitored at 655 nm (see Figure 11B). The resolution of two emission peaks at low temperature is possibly due to vibrational narrowing of the emission lines and is consistent with a significant molecular weight distribution in the sample (see GPC results above and solubility properties). The PL data of the PBTPI in solution at room temperature are comparable to those of PBTPV[20] (555 nm), PPV[36] (550 nm), and PDBTT[24b] (557 nm).

Thermal Analysis. The thermal stability of the polymer in its various forms was examined by TGA. The onset of thermal decomposition of PBTPI is 370 °C in flowing nitrogen and 330 °C in flowing oxygen. By comparison, the onset of thermal decomposition of PPI is 504 °C in flowing nitrogen.[19] The observed thermal stability of PBTPI is lower than that of PPI as would

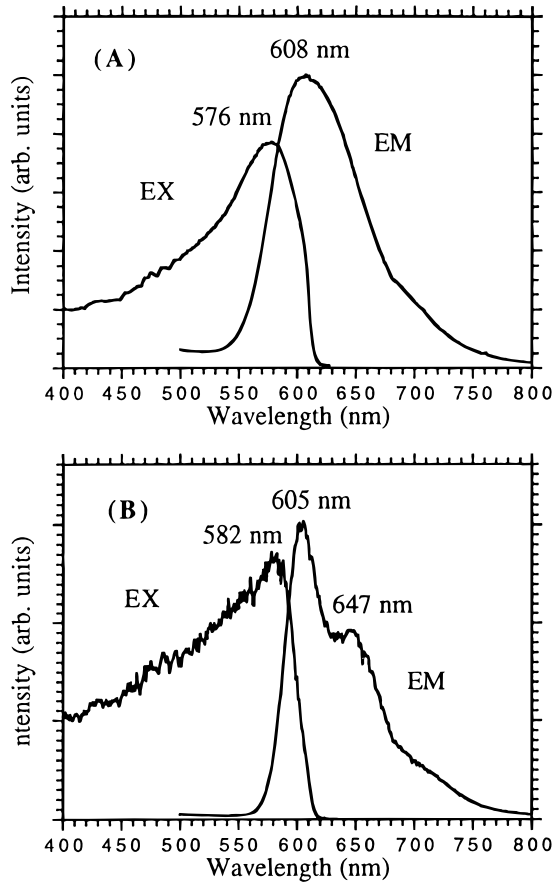

Figure 11. Photoluminescence spectra of bulk PBTPI solid at (A) 300 and (B) 77 K.

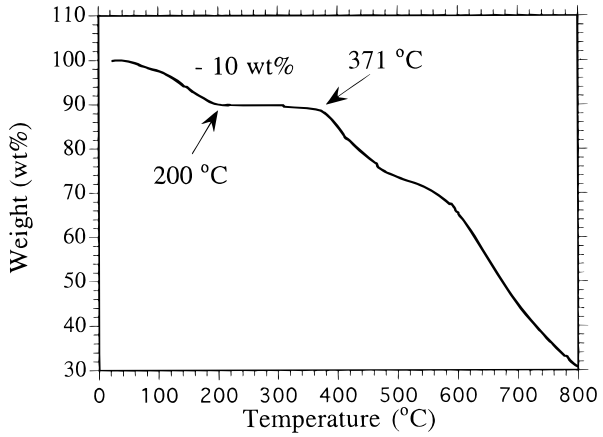

Figure 12. TGA thermogram of protonated (with HCl) bulk PBTPI under nitrogen flow.

be expected, given the presence of the flexible pendant butyl groups in the former. In spite of this, PBTPI has a reasonably good thermal stability, comparable to its isoelectronic analog PBPTV (378 °C under nitrogen)[20] and to the homopolythiophene poly(DBTT) (380 °C under nitrogen).[24b] Figure 12 shows the thermogram of the protonated polymer under nitrogen. By comparison with the neutral polymer, the weight loss from 54 to 200 °C is assigned to the weight loss of HCl (deprotonation process). Above 200 °C, the TGA profile is very similar to that of the neutral polymer. From the weight loss due to HCl, we estimate the level of protonation of the polymer to be ~1.5 per repeating unit (each repeat unit has two possible protonation sites). This result is in good agreement of the EDS/SEM microprobe analysis of the sulfur to chlorine ratio of 4.3. These results

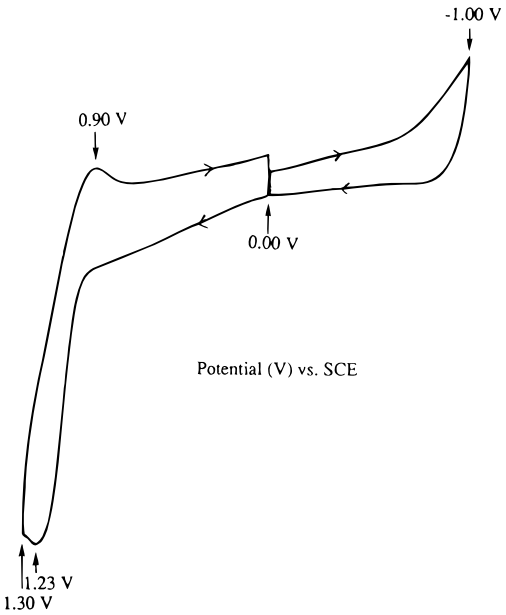

Figure 13. Typical cyclic voltammogram of a solution-cast PBTPI film on a Pt electrode in CH_3CN−0.1 M $(Bu_4N)ClO_4$. Scan rate, 20 mV/s.

suggest that 25% of the nitrogen sites are not protonated. Differential scanning calorimetry analysis of the neutral polymer showed no evidence of a measurable glass transition or melting point in the range of 30−330 °C.

Electron Spin Resonance (ESR) Spectroscopy. The structural homogeneity of the neutral and protonated polymers was probed by ESR spectroscopy. Both materials give very weak ESR signals with the same g value of 2.0040 and ΔH_{pp} of 7.6 and 8.5 G for the neutral and protonated polymers, respectively. The spectra also show that the protonation of PBTPI did not increase the number of spins in the polymer. Because of the extreme weakness of the signals, we judge that both forms of the polymer contain few structural defects.

Electrochemistry. The redox properties of both neutral and protonated PBTPI were investigated by cyclic voltammetry. PBTPI thin films were solution-cast onto a Pt plate as a working electrode. Figure 13 shows a typical cyclic voltammogram (CV) of the neutral polymer film in acetonitrile solution containing 0.1 M Bu_4NClO_4. The first negative (cathodic) scan from 0.0 to −1.0 V vs SCE was featureless and the film remained orange. During the first anodic cycle from 0.0 to +1.4 V, the as-deposited orange thin film on the Pt electrode turned blue after oxidation at 1.23 V and remained blue after reduction at 0.90 V. Further scans between −1.0 and 1.4 V did not show well-defined redox waves. Figure 14 shows a CV of the blue protonated film (prepared by exposing the red neutral film to HCl vapor) in acetonitrile solution containing 0.1 M Bu_4NClO_4. The first negative scan from 0.0 to −1.0 V shows a broad cathodic wave at −0.69 V vs SCE, which may be due to the reduction of protons to hydrogen. After the negative scan, the film turned orange. Further repetitive cathodic scans from 0.0 to −1.0 V result in a decrease of the cathodic current, while the film stays orange. Then, the following first anodic scan from 0.0 to 1.2 V turned the film to blue and showed an anodic peak at 1.10 V and a cathodic peak at 1.06 V. Further scans from 0.0 to 1.4 V did not show well-defined redox waves, same as the unprotonated form. These results suggest that during the first cathodic scan the protonated form

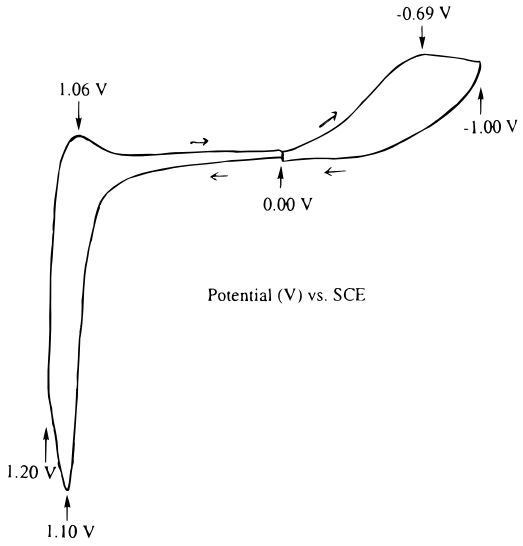

Figure 14. Typical cyclic voltammogram of a solution-cast PBTPI film protonated with HCl on a Pt electrode in CH_3CN−0.1 M $(Bu_4N)ClO_4$. Scan rate, 20 mV/s.

converts to the initial orange form due to the depletion of available protons. The detailed elucidation of the electron- or proton-transfer process of the neutral and protonated forms of PBTPI needs further investigation.

Electrical Conductivity. The electrical conductivities of iodine-doped polymers (both the neutral and protonated materials) and the undoped materials were measured by the standard four-probe method on pressed pellets at room temperature. Both the neutral and protonated polymers are insulators ($\sigma \sim 10^{-9}-10^{-10}$ S/cm). Both the iodine-doped materials have conductivities of $10^{-7}-10^{-8}$ S/cm. These conductivities are much lower than those of reported poly(Schiff bases) ($\sigma \sim 10^{-3}-10^{-4}$ S/cm),[16b] probably due to the fact that the polymer is difficult to oxidize, as suggested by the CV studies mentioned above.

Concluding Remarks

A new derivative of conjugated aromatic poly(azomethine) containing the alkyl-substituted oligothiophene was prepared under ethanothermal reaction conditions. The resulting polymer, PBTPI, has improved solubility in organic solvents as imparted by the dibutyl-substituted terthiophene linkages on the polymer backbone. Replacement of a phenylene linkage by an oligothiophene linkage in the poly(azomethine) backbone enhanced the π-electron delocalization of the polymer and resulted in a significant reduction in band gap by ~0.4 eV. The new poly(azomethine), PBTPI, has an optical band gap of 2.06 eV, which is the lowest among conjugated aromatic poly(azomethines) and comparable to its isoelectronic (all-carbon backbone) counterpart PBTPV. However, unlike PBTPV, the incorporation of imine nitrogen on the polymer backbone provides Lewis base sites for effecting reversible protonation and complexation. Thus, PBTPI is completely soluble in concentrated sulfuric acid and nitromethane containing Lewis acids (e.g., $AlCl_3$). Protonation is very facile and reversible, causes the color of the polymer to change from red to blue, and reduces the band gap to 1.61 eV. This band gap narrowing is attributed to the strong electron-withdrawing effect of the protons attached to the imine nitrogen. The electrical conductivity of the iodine-doped PBTPI remains low in the order of $10^{-7}-10^{-8}$ S/cm. The reactivity of the polymer with strong acids and the low band gap of the protonated form may have potential applications in solid-state acid indicators and photonic materials.

Acknowledgment. Financial support from the National Science Foundation (DMR-93-06385) and the Center for Fundamental Materials Research at Michigan State University is gratefully acknowledged. We thank Professor C. K. Chang for fruitful discussions.

References and Notes

(1) (a) Bredas, J. L., Chance, R. R., Eds. *Conjugated Polymeric Materials: Opportunities in Electronics, Optoelectronics, and Molecular Electronics*; Kluwer Academic Publishers: Dordrecht, The Netherlands, 1990. (b) Skotheim, T. A., Ed. *Handbook of Conducting Polymers*; Marcel Dekker: New York, 1986. (c) Kanatzidis, M. G. *Chem., Eng. News* **1990,** *68*, (Dec 3), 36−54. (d) Roncali, J. *Chem. Rev.* **1992**, *92*, 711

(2) Prasad, P. N.; Williams, D. J. *Introduction to Nonlinear Optical Effects in Molecules and Polymers*; Wiley: New York, 1991.

(3) (a) Su W. P.; Schrieffer, J. R.; Heeger, A. *J. Phys. Rev. Lett.* **1979**, *42*, 1698−1701. (b) Park, Y. W.; Heeger, A. J.; Druy, M. A.; MacDiarmid, A. G. *J. Chem. Phys.* **1980**, *73*, 946−957.

(4) Frommer, J. E.; Chance, R. R. *Encyl. Polym. Sci. Eng.* **1985**, *5*, 462−507.

(5) (a) Antoun, S.; Karasz, F. E.; Lenz, R. W. *J. Polym. Sci., Part A: Polym. Chem.* **1988**, *26*, 1800−1817. (b) Eckhardht, H.; Shacklette, L. W.; Jen, K. Y.; Elsenbaumer, R. L. *J. Chem. Phys.* **1989**, *91*, 1301−1315.

(6) (a) Chiang, J, C.; MacDiarmid, A. G. *Synth. Met.* **1986**, *13*, 193. (b) Epstein, A., J.; Ginder, J. M.; Zuo, F.; Bigelow, R. W.; Woo, H.-S.; Tanner, D. B.; Richter, A. F.; Huang, W. S.; MacDiarmid, A. G. *Synth. Met.* **1987**, *18*, 303−309.

(7) (a) Astruias, G. E.; MacDiarmid, A. G.; McCall, R. P.; Epstein, A., J. *Synth. Met.* **1989**, *29*, E157−E163. (b) Sun, Y.; MacDiarmid, A. G.; Epstein, A., J. *J. Chem. Soc., Chem. Commun.* **1990**, 529−531. (c) Huang, W. S.; MacDiarmid, A. G.; Epstein, A., J. *J. Chem. Soc., Chem. Commun.* **1987**, 1784−1785.

(8) Hauer, C. R.; King, G. S.; McCool, E. L.; Euler, W. B.; Ferrara, J. D.; Youngs, W. J. *J. Am. Chem. Soc.* **1987**, *109*, 5760−5765.

(9) Cao, Y.; Li, S. *J. Chem. Soc., Chem. Commun.* **1988**, 937.

(10) (a) Euler, W. B.; Roberts, J. E. *Synth. Met.* **1989**, *29*, E546. (b) Chaloner-Gill, B.; Cheer, C. J.; Roberts, J. E.; Euler, W. B. *Macromolecules* **1990**, *23*, 4597. (c) Chaloner-Gill, B.; Euler, W. B.; Roberts, J. E. *Macromolecules* **1991**, *24*, 3074−3080.

(11) Adams, R.; Bullock, J. E.; Wilson, W. C. *J. Am. Chem. Soc.* **1923**, *45*, 521.

(12) D'Alelio, G. F.; Schoenig, R. K.; *J. Macromol. Sci. Rev.: Macromool. Chem.* **1969**, *C3*, 105−234.

(13) Morgan, P. W.; Kwolek, S. L.; Pletcher, T. C. *Macromolecules* **1987**, *20*, 729−739.

(14) (a) Millaud, B.; Thierry, A.; Skoulios, A. *Mol. Cryst. Liq. Cryst. Lett.* **1978**, *41*, 263. (b) Noel, C.; Billard, J. *Mol. Cryst. Liq. Cryst. Lett.* **1978**, *41*, 260−262.

(15) (a) Yang, C.-J.; Jenekhe, S. A. *Macromolecules* **1995**, *28*, 1180−1196. (b) Jenekhe, S. A.; Yang, C.-J.; Vanherzeele, H.; Meth, J. S. *Chem. Mater.* **1991**, *3*, 987−989.

(16) (a) Barbarin, F.; Blance, J. P.; Dugay, M.; Fabre, C.; Maleysson, C. *Synth. Met.* **1984/85**, *10*, 71−78. (b) Li, X.; Li, C.; Li, S. *Synth. Met.* **1993**, *60*, 285−288.

(17) Lee, K. S.; Won, J. C.; Jung, J. C. *Makromol. Chem.* **1989**, *190*, 1547−1552.

(18) Park, S.-B.; Kim, H.; Zin, W.-C.; Jung, J. C. *Macromolecules* **1993**, *26*, 1627−1632.

(19) (a) Jenekhe, S. A.; Yang, C.-J. *Chem. Mater.* **1991**, *3*, 878−887. (b) Yang, C.-J.; Jenekhe, S. A. *Chem. Mater.* **1994**, *6*, 196−203.

(20) (a) Wang, C.; Xie, X.; LeGoff, E.; Albritton-Thomas, J.; Kannewurf, C. R.; Kanatzidis, M. G. *Synth. Met.* **1995**, *74*, 71−74. (b) Wang, C.; Shieh, S.; LeGoff, E.; Kanatzidis, M. G., manuscript in preparation.

(21) Ethanothermal conditions, i.e., ethanol medium over 120 °C and autogenous pressure.

(22) During preparation of this paper, a poly(azomethine) constituted of six thienylene and two phenylene segments

linked together with azomethines moieties was briefly described in the literature: Destri, S; Masecherpa, M.; Porzio, W. *Synth. Met.* **1995**, *69*, 287−288.
(23) Agrawal, A. K.; Jenekhe, S. A. *Macromolecules* **1993**, *26*, 895−905.
(24) (a) Wang, C.; Benz, M. E.; LeGoff, E.; Schindler, J. L.; Kannewurf, C. R.; Kanatzidis, M. G. *Polym. Prepr.* **1993**, *34* (2), 422−423. (b) Wang, C.; Benz, M. E.; LeGoff, E.; Schindler, J. L.; Albritton-Thomas, J.; Kannewurf, C. R.; Kanatzidis, M. G. *Chem. Mater.* **1994**, *6*, 401−411.
(25) Hydrothermal conditions, i.e., aqueous medium over 100 °C and autogenous pressure. (a) Rabenau, A. *Angew. Chem., Int. Ed. Engl.* **1985**, *24*, 1026−1040. (b) Haushalter, R. C.; Mundi, L. A. *Chem. Mater.* **1992**, *4*, 31−48. (c) Liao, J.-H.; Kanatzidis, M. G. *J. Am. Chem. Soc.* **1990**, *112*, 7400−7402. (d) Liao, J.-H.; Kanatzidis, M. G. *Inorg. Chem.* **1992**, *31*, 431−439.
(26) Cerius^2 1.6 software package by Molecular Simulations Inc., San Diego, CA.
(27) Liao, J.-H.; Benz, M.; LeGoff, E.; Kanatzidis, M. G. *Adv. Mater.* **1994**, *6*, 135−138.
(28) It is known that a partially amorphous material usually has lower density than the fully crystalline version of the material: Mo, Z.; Lee, K.-B.; Moon, Y. B.; Kobayashi, M.; Heeger, A. J.; Wudl, F. *Macromolecules* **1985**, *18*, 1972−1977.
(29) (a) Jenekhe, S. A.; Johnson, P. O.; Agrawal, A. K. *Macromolecules* **1989**, *22*, 3216−3222. (b) Jenekhe, S. A.; Johnson, P. O. *Macromolecules*, **1990**, *23*, 4419−4429. (c) Roberts, M. F.; Jenekhe, S. A. *Polym. Commun.* **1990**, *31*, 215−217. (d) Osaheni, J. A.; Jenekhe, S. A. *Chem. Mater.* **1992**, *4*, 1282−1290.
(30) Socrates, G. *Infrared Characteristic Group Frequencies*; John Wiley & Sons: New York, 1994.
(31) Maior, R. M.; Hinkelmann, K.; Eckert, H.; Wudl. F. *Macromolecules* **1990**, *23*, 1268−1279.
(32) (a) Ward, B.; Chang, C. K.; Young, R. *J. Am. Chem. Soc.* **1984**, *106*, 3943−3950. (b) Hanson, L. K.; Chang, C. K.; Ward, B.; Callahan, P. M.; Babcock, G. T.; Head, J. *J. Am. Chem. Soc.* **1984**, *106*, 3950−3958.
(33) Bakhshi, A. K.; Liegener, C.-M.; Ladik, J. *Synth. Met.* **1989**, *30*, 79−85.
(34) (a) Wendlandt, W. W.; Hecht, H. G. *Reflectance Spectroscopy*; Interscience Publishers: New York, 1966. (b) Kotum, G. R. *Reflectance Spectroscopy*; Springer Verlag: New York, 1969. (c) Tandon, S. P.; Gupta, J. P. *Phys. Status Solid* **1970**, *38*, 363−367.
(35) These values are obtained by extrapolating the linear portions of the square of the absorption coefficient, $(\alpha/S)^2$ vs E plots to $(\alpha/S)^2 \rightarrow 0$.
(36) (a) Hay, M. F.; Yang, Y.; Klavetter, F. L. *Polym. Prepr. (Am. Chem. Soc., Div. Polym. Chem.)* **1994**, *35* (1), 293−294. (b) Yang, Z.; Sokolik, I.; Karasz, F. E. *Macromolecules* **1993**, *26*, 1188−1190.

MA9514131